Experimental

Chemicals: Vanadyl sulfate pentahydrate (purum, Fluka), TEOS (98 %, Fluka), hydrogen peroxide (30 %, Perhydrol, p.a., Merck), ammonia (25 %, p.a., Merck), isopropanol (99.5 %, J. T. Baker) were used as purchased.

Synthesis: Fibrous $V_3O_7{\cdot}H_2O$ template crystals were prepared hydrothermally according to Yamamoto and co-workers [30]: an aqueous solution of $VOSO_4$ (0.15 M) was sealed in a poly(tetrafluoroethylene)-lined autoclave (Parr bomb 4749, 23 mL capacity) and heated at 180–220 °C for 1–2 days. The resulting suspension was filtered, washed several times with water and dried overnight under vacuum ($\sim 10^{-3}$ mbar). Coating of the as-prepared green, paper-like template as well as the subsequent core removal were performed in one pot. The fibrous solid (35 mg) was dispersed in a 250 mL glass flask containing an isopropanol/ammonia/water solution (respective volumes [mL]: 200:8.3:7.5) by means of an ultrasonic bath set at 40 °C (Bandelin Sonorex DK 255 P apparatus, 35 kHz, 320 W). After addition of 0.1 mL TEOS, the ultrasound intensity was maintained at ~200 W during the whole coating reaction (75 min). Then, 1 mL H_2O_2 was added directly into the dispersion, which was further stirred for about 45 min. The solid was collected by filtration, washed extensively with isopropanol, and afterwards with water. To achieve complete core dissolution as well as elemental purity, the product was redispersed in a diluted H_2O_2 aqueous solution (0.3 M; 30 mL), stirred for 48 h, washed several times with water, and dried under vacuum.

Characterization: Samples were investigated in glass capillaries with a STOE STADI P X-ray powder diffractometer equipped with a curved Ge monochromator, a linear position sensitive detector, and using Cu Kα radiation. Scanning electron microscopy (SEM) was performed on a LEO 1530 Gemini apparatus, which was operated at low acceleration voltage ($V_{acc} = 1$ kV) to minimize charging of the as-synthesized samples. For transmission electron microscopy (TEM), the samples were deposited on a holey carbon foil supported on a copper grid. TEM images were recorded on a CM30 microscope (Philips, Eindhoven, $V_{acc} = 300$ kV, LaB_6 cathode). Elemental maps of vanadium were obtained at the L ionization edge applying the three-window method [33] on a Tecnai 30F apparatus (Philips, Eindhoven, $V_{acc} = 300$ kV, field emission gun) equipped with a GIF (Gatan imaging filter). Laser elemental analysis was carried out on a pressed sample pellet using a Perkin Elmer/Sciex Elan 6100 DRC LA-ICP-MS machine.

Received: March 20, 2003
Final version: June 5, 2003

[1] S. Iijima, *Nature* **1991**, *354*, 56.
[2] W. Tremel, *Angew. Chem. Int. Ed.* **1999**, *38*, 2175.
[3] R. Tenne, *Prog. Inorg. Chem.* **2001**, *50*, 269.
[4] G. R. Patzke, F. Krumeich, R. Nesper, *Angew. Chem. Int. Ed.* **2002**, *41*, 2446.
[5] Y. Konishi, M. Okazaki, K. Toriyama, T. Kasai, *J. Phys. Chem. B* **2001**, *105*, 9101.
[6] J. L. Gole, M. G. White, *J. Catal.* **2001**, *204*, 249.
[7] A. Hanprasopwattana, S. Srinivasan, A. G. Sault, A. K. Datye, *Langmuir* **1996**, *12*, 3173.
[8] M. Quobosheane, S. Santra, P. Zhang, W. Tan, *Analyst* **2001**, *126*, 1274.
[9] J. Livage, T. Coradin, C. Roux, *J. Phys.: Condens. Matter* **2001**, *13*, R673.
[10] T. K. Jain, I. Roy, T. K. De, A. Maitra, *J. Am. Chem. Soc.* **1998**, *120*, 11 092.
[11] H. J. Chang, Y. F. Chen, H. P. Lin, C. Y. Mou, *Appl. Phys. Lett.* **2001**, *78*, 3791.
[12] M. Zhang, E. Ciocan, Y. Bando, K. Wada, L. L. Cheng, P. Pirouz, *Appl. Phys. Lett.* **2002**, *80*, 491.
[13] L. L. Hench, J. K. West, *Chem. Rev.* **1990**, *90*, 33.
[14] R. A. Caruso, M. Antonietti, *Chem. Mater.* **2001**, *13*, 3272.
[15] J. H. Jung, Y. Ono, S. Shinkai, *Langmuir* **2000**, *16*, 1643.
[16] F. Kleitz, U. Wilczok, F. Schüth, F. Marlow, *Phys. Chem. Chem. Phys.* **2001**, *3*, 3486.
[17] S. M. Yang, I. Sokolov, N. Coombs, C. T. Kresge, G. A. Ozin, *Adv. Mater.* **1999**, *11*, 1427.
[18] S. Baral, P. Schoen, *Chem. Mater.* **1993**, *5*, 145.
[19] Y. Ono, Y. Kanekiyo, K. Inoue, J. Hojo, M. Nango, S. Shinkai, *Chem. Lett.* **1999**, 475.
[20] W. Shenton, T. Douglas, M. Young, G. Stubbs, S. Mann, *Adv. Mater.* **1999**, *11*, 253.
[21] H. Nakamura, Y. Matsui, *J. Am. Chem. Soc.* **1995**, *117*, 2651.
[22] F. Miyaji, S. A. Davis, J. P. H. Charmant, S. Mann, *Chem. Mater.* **1999**, *11*, 3021.
[23] L. Wang, S. Tomura, F. Ohashi, M. Maeda, M. Suzuki, K. Inukai, *J. Mater. Chem.* **2001**, *11*, 1465.
[24] B. C. Satishkumar, A. Govindaraj, E. M. Vogl, L. Basumallick, C. N. R. Rao, *J. Mater. Res.* **1997**, *12*, 604.
[25] C. R. Martin, *Science* **1994**, *266*, 1961.
[26] B. B. Lakshmi, C. J. Patrissi, C. R. Martin, *Chem. Mater.* **1997**, *9*, 2544.
[27] F. Schlottig, M. Textor, U. Georgi, G. Roewer, *J. Mater. Sci. Lett.* **1999**, *18*, 599.
[28] M. Zhang, Y. Bando, K. Wada, *J. Mater. Res.* **2000**, *15*, 387.
[29] C. Hippe, M. Wark, E. Lork, G. Schulz-Ekloff, *Microporous Mesoporous Mater.* **1999**, *31*, 235.
[30] Y. Oka, T. Yao, N. Yamamoto, *J. Solid State Chem.* **1990**, *89*, 372.
[31] Joint Committee on Powder Diffraction Standards (JCPDS), International Centre for Diffraction Data (ICDD), card No. 28–1433 ($V_3O_7{\cdot}H_2O$).
[32] W. Stöber, A. Fink, E. Bohn, *J. Colloid Interface Sci.* **1968**, *26*, 62.
[33] L. Reimer, *Energy-Filtering Transmission Electron Microscopy*, Springer, Berlin **1995**, p. 347.

Functional Molecularly Imprinted Polymer Microstructures Fabricated Using Microstereolithography**

By *Peter G. Conrad II*, *Peter T. Nishimura*, *Damian Aherne*, *Benjamin J. Schwartz*, *Dongmin Wu*, *Nicholas Fang*, *Xiang Zhang*, *M. Joseph Roberts*, and *Kenneth J. Shea**

A defining trend in sensing and diagnostics is miniaturization, the reduction in the size of devices and components to micrometer or submicrometer length scales.[1–4] More compact devices have lower power demands and the potential for a greater economy of production. Applications for micro-devices are numerous and include implantable medical biosensors,[5–11] drug-screening devices,[12] and microelectromechanical systems (MEMS).[1,13–15] Microfabrication technology can achieve rapid assembly of the electrical and mechanical components of these devices. However, the introduction of additional function, such as molecular recognition to identify or concentrate biological analytes, requires "soft" materials. These "soft" materials are typically not compatible with direct lithographic techniques and thus their introduction is achieved in subsequent steps of device fabrication. In addition to the obvious advantages of simplification of the fabrication process, compatible functionalization procedures could

[*] Prof. K. J. Shea, Dr. P. G. Conrad II
Department of Chemistry, University of California
Irvine, CA 92697-2025 (USA)
E-mail: KJShea@uci.edu
Dr. P. T. Nishimura, Dr. D. Aherne, Prof. B. J. Schwartz
Department of Chemistry and Biochemistry, University of California
Los Angeles, CA 90095-1569 (USA)
Dr. D. Wu, Dr. N. Fang, Prof. X. Zhang,
Department of Mechanical and Aerospace Engineering
University of California
Los Angeles, CA 90095-1569 (USA
Dr. M. J. Roberts
NAVAIR NAWCWD, Polymer Science and Engineering Branch
China Lake, CA 93555 (USA)

[**] The authors are grateful to DARPA for financial support. Research in the KJS lab is partially supported by the National Institute of Health. BJS is a Cottrell Scholar of Research Corporation, an Alfred P. Sloan Foundation Research Fellow, and a Camille Dreyfus Teacher-Scholar. Microstereolithography work at the XZ lab is partially funded by NSF CAREER Award and ONR Young Investigator Award.

ADVANCED MATERIALS

further expand the utility and scope of micro devices. For a lithographic approach, this would require methods to produce spatially resolved, micrometer-sized features of functional materials capable of molecular recognition.

Of the many strategies for creating synthetic receptors, molecular imprinting, a method for making robust crosslinked polymers with recognition sites for complex organic molecules, offers a number of advantages for this application.[16–20] Molecularly imprinted polymers (MIPs) are typically thermosets generated by polymerization of fluid solutions of monomers. Importantly, the approach is generally offering the opportunity for fabricating receptors for a variety of molecular structures. Furthermore, the imprinted photopolymers containing recognition sites are capable of withstanding a variety of solvents and temperature extremes.[16–20] The integration of imprinted polymers into micro-sensors and diagnostic devices requires procedures for fabricating MIPs in two- and three-dimensional (2D and 3D) patterns. Methods for producing these structures include simple lithography, microcontact printing (soft lithography),[21–23] microstereolithography (μSL), and 2-photon-3D lithography.[24] There have been very few reports of micropatterned functional MIPs. A notable exception is the work of Yan and Kapua, who reported fabrication of imprinted micrometer-sized features using soft lithography.[21]

In this communication, we report the use of μSL for fabricating imprinted 3D microstructures capable of recognizing a targeted analyte. The imprinting procedure should, with some modification, be applicable to many standard lithographic methods.

μSL is a method for manufacturing complex 3D shapes by means of localized photopolymerization using a sharply focused laser beam.[25] μSL was first reported in 1993 utilizing principles based on stereolithography to fabricate macro-sized models.[26] A computer-assisted design (CAD) program is used to horizontally slice the desired 3D image into 2D layers. A directed UV laser beam is focused to 1–2 μm onto the surface of a glass microscope slide coated with a thin layer of a liquid monomer solution, resulting in localized photopolymerization; synchronized motion of the substrate in the x–y plane is then used to fabricate the pattern of the lowest 2D slice.[25,27] Translation along the z-axis allows the next layer to be "written" on top of the first. Repetition of these steps allows complex and intricate microstructures to be built layer by layer.

To achieve spatial resolution, it is necessary to control the effective area of localized photopolymeriztion, which determines the height, or "curing depth", of each of the polymerized layers. Jacobs[28] established a working curve for controlling the curing depth in μSL based on the photopolymer's threshold exposure. The curing depth (C_d) depends, in part, on the concentration and molar extinction coefficients of the initiator and an additional UV-absorber (UVA).

For the integration of μSL and imprinting we elected to fabricate well-defined, micrometer-sized structures with adenine recognition.[29] Adenine was chosen because of the occurrence of this fragment in many biologically important molecules and the considerable information available regarding the preparation and evaluation of molecularly imprinted synthetic adenine receptors.[29–31] An imprinting formulation developed for μSL is shown in Figure 1. The components include 9-ethyl adenine (9-EA, **1**, the imprint molecule) and methacrylic acid (MAA, **2**, the functional monomer) in concentrated chloroform solution.[30] The high degree of crosslinking, a requirement for imprinting,[32] was achieved by incorporation of the trifunctional crosslinker trimethylolpropane trimethacrylate (TRIM, **4**). The choice of photoinitiator and UVA additive was dictated by absorption wavelength, quantum efficiency,

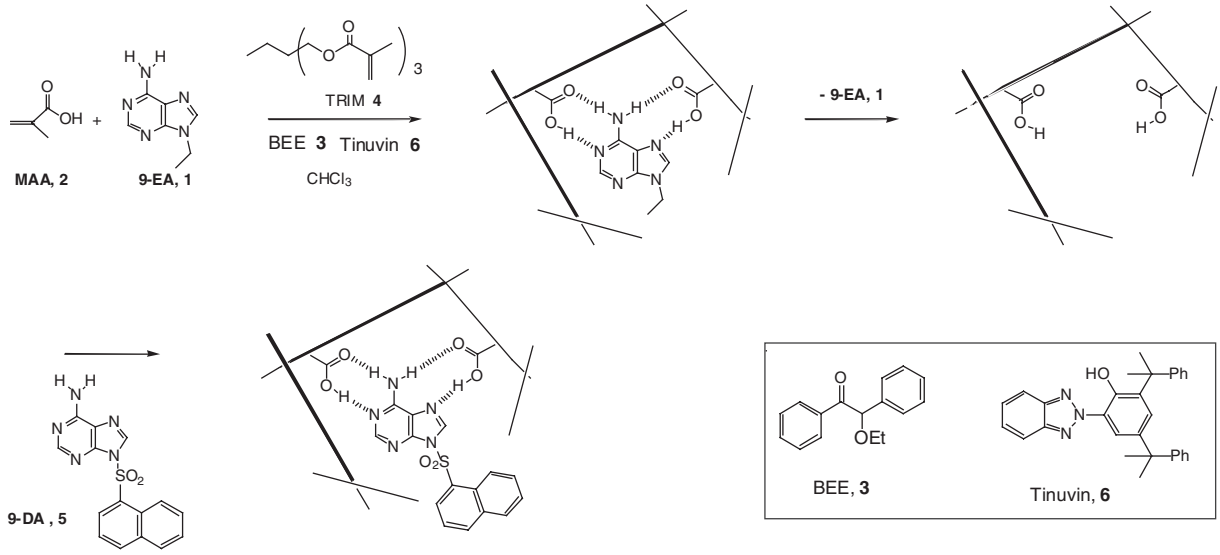

Fig. 1. Scheme depicting the fabrication of adenine selective molecularly imprinted polymers and subsequent absorption of the adenine derivative, 9-dansyl adenine, **5**. 9-Ethyl adenine, **1**, serves as the template with methacrylic acid, **2**, as the functional monomer, while TRIM, **4**, functions as a crosslinking agent. Benzoin ethyl ether, **3**, is utilized as the initiator for μSL procedures, and Tinuvin, **6**, is added as a UVA to achieve curing depth resolution. 9-Dansyl adenine, **5**, functions as a fluorescent probe to analyze the binding sites in the resulting microstructure.

and compatibility with the formation of a functional MIP. After considerable experimentation (vide infra), benzoin ethyl ether (BEE, **3**, $\lambda = 354$ nm ($\varepsilon = 509$ M^{-1} cm^{-1})), and Tinuvin, **6**, were chosen as the photoinitiator and the UVA additive, respectively. Tinuvin (**6**) possesses a large molar absorptivity coefficient (151 600 M^{-1} cm^{-1}) at 364 nm (the photopolymerization wavelength employed) and was found to be effective in achieving low curing depths (high z spatial resolution).

The evaluation of imprinted polymers prepared by bulk polymerization is traditionally conducted using high-pressure liquid chromatography (HPLC) techniques. However, with micrometer-sized objects, the number of binding sites is below the detection limits of HPLC analysis. We have developed an assay that utilizes the fluorescence emission of a dansyl-tagged adenine derivative to evaluate binding to microfabricated structures. Polymers imprinted with 9-EA display an affinity for a number of adenine derivatives bearing substituents at the 9-position.[29–31] The adenine specificity is not compromised by these substituents. The primary binding interactions between adenine derivatives and the carboxylic acid functional groups on the imprinted polymer are believed to be Watson–Crick and Hoogstein H-bonding interactions on the basic residues of the "upper portion" of the adenine molecule.[30] These recognition elements allow considerable freedom in substitution at the 9-position ("lower portion") while maintaining overall adenine specificity by the MIP. A fluorescent analog, 9-dansyl adenine (9-DA, **5**), was synthesized for this purpose.[33] Independent evaluation of the affinity of 9-EA imprinted polymers towards 9-DA was established in bulk polymer experiments.

To verify that the choice of **3** as a photoinitiator and **6** as a UVA does not interfere with the imprinting process or create additional non-specific binding interactions, a variety of non-patterned test samples were prepared. Their composition is summarized in Table 1. Each of the four solution mixtures (**S1**–**S4**) was dip-coated onto glass microscope slides previously silylated with 3-(trimethyoxysilyl)propyl methacrylate, allowing for better adhesion of the photodeposited polymer to the glass substrates.

The polymers were grown by light exposure in a UV-chamber for 5 min then washed in chloroform for 12 h to remove 9-EA, **6**, **3**, and any unreacted monomers. The washing protocol of these non-covalent imprinted polymers has been shown to quantitatively remove template molecules.[29–31] These unpatterned samples were then bathed in a 1×10^{-5} M solution of 9-DA in chloroform. The 9-DA absorbed in the samples was excited using the 488 nm line from an Ar^+ laser (a wavelength chosen to avoid absorption by any residual **6**), and ~600 nm dansyl fluorescence from the samples was imaged through a 530 nm long pass filter onto a charge coupled device (CCD) camera. Integration of the fluorescent image was plotted as a function of time and demonstrates that the additional reagents required for μSL do not interfere with the binding interactions between functional monomer and template during the polymerization process. Additionally, the reagents do not provide an increase in non-specific binding sites.

Having established imprinting formulations for patterning we next devoted our attention to the micropatterning of functional polymers via μSL. First, 2D patterns were fabricated to verify that the patterned microstructures show similar selectivity to the bulk polymers. 2D grids were prepared from the UV-curable MIP and control UV-curable solutions (**S1** and **S3**, respectively) using the 364 nm line of the Ar^+ laser and an x–y–z motorized stage. Figure 2 shows an image of the resulting pattern, which has an overall dimension of 600 μm × 600 μm; the width of the lines comprising the grid is < 20 μm.

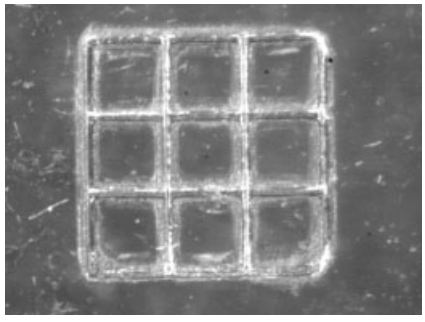

Fig. 2. 2D microstructure (600 μm × 600 μm) fabricated by μSL from solution **S1**.

After fabrication, the micropatterned polymers were washed thoroughly with isopropyl alcohol and then chloroform. This procedure is based upon bulk polymer studies to insure complete template removal. Uptake studies were performed by bathing both the imprinted and control structures in 9-DA chloroform solutions (1.8×10^{-4} M) and measuring the total fluorescence from each sample as a function of time. The 2D patterned MIP showed a 5:1 preference for 9-DA over the control polymer, a value comparable to previous reports for 9-EA MIPs prepared under bulk conditions.[30]

With the success of 2D photopatterned MIPs, the next step was to produce functional 3D structures. Based on curing depth analysis experiments, the curing depth of the polymerization solutions was estimated to be ~20 μm. Thus, to fabricate 3D structures, we lowered the z-axis of the translation stage by 20 μm after the x–y scan of each 2D "slice" was com-

Table 1. Composition of solutions used during polymerization procedures. Chloroform and TRIM were purified by flashing through an alumina column, while 9-ethyl adenine was flash chromatographed on a silica column. Methacrylic acid was freshly distilled prior to use. Tinuvin and benzoin ethyl ether were used as received. Solutions were prepared freshly prior to use, and stored in an amber bottle to keep from incident light.

Substrate	S1	S2	S3	S4
Chloroform	6.271 g	6.271 g	6.271 g	6.271 g
TRIM	6.274 g	6.274 g	6.274 g	6.274 g
Methacrylic acid	0.327 g	0.327 g	0.327 g	0.327 g
Tinuvin	0.013 g	–	0.013 g	–
Benzoin ethyl ether	0.131 g	0.131 g	0.131 g	0.131 g
9-Ethyl adenine	0.050 g	0.050 g	–	–

ADVANCED MATERIALS

pleted. After building up multiple 2D layers, the resulting 3D polymer objects had a total height of approximately 100 μm; scanning electron micrographs of the 3D "waffle pattern" produced in this fashion are shown in Figure 3.

As with the unpatterned and 2D patterned polymers, rebinding studies were conducted for both the MIP and control 3D structures. The 3D structures were rinsed and bathed in chloroform for 12 h to wash the 9-EA template and any unreacted materials from the MIP. The structures were then exposed to a solution of 9-DA (1.08×10^{-4} M in chloroform) for increasing time intervals, gently rinsed to remove any residual 9-DA, and fluorescently imaged. The results are shown in Figure 4.

An approximate 4.5-fold increase in fluorescent intensity compared to the control polymer **S3** was observed in the imprinted structure **S1**. These results indicate that the 3D microstructures exhibit affinity for 9-DA comparable to that of the 2D and bulk imprinted materials.

In summary, we have demonstrated the ability to fabricate functionalized, three-dimensional molecularly imprinted microstructures using μSL. Microstructures with recognition for adenine and its derivatives have been prepared. The experimental conditions used to achieve spatial resolution in μSL do not disrupt the binding interactions between the functional monomers and the template. The range of target analytes that are responsive to molecular imprinting is large and includes simple drugs and their metabolites, pesticides, peptides, and proteins. These techniques will allow for the direct integration of functional polymers with molecular recognition into the microfabrication process.

Received: November 11, 2002
Final version: June 10, 2003

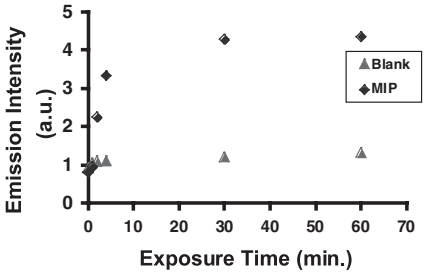

Fig. 4. Rebinding isotherm (fluorescence intensity as a function of exposure time to a 1.08×10^{-4} M solution of 9-DA in chloroform) for both 9-EA-imprinted (MIP) and control (blank) 3D microstructures as those presented in Figure 3.

[1] R. Mariella Jr., *Biomed. Microdevices* **2002**, *4*, 77.
[2] M. J. O'Donnell-Maloney, D. P. Little, *Genet. Anal.: Biomol. Eng.* **1996**, *13*, 151.
[3] J. Wang, F. Lu, L. Angnes, J. Liu, H. Sakslund, Q. Chen, M. Pedrero, L. Chen, O. Hammerich, *Anal. Chim. Acta* **1995**, *305*, 3.
[4] W. E. Morf, N. F. de Rooij, *Sens. Actuators, A* **1995**, *A51*, 89.
[5] Z. A. Strong, A. W. Wang, C. F. McConaghy, *Biomed. Microdevices* **2002**, *4*, 97.
[6] R. Hintsche, M. Paeschke, U. Wollenberger, U. Schnakenberg, B. Wagner, T. Lisec, *Biosens. Bioelectron.* **1994**, *9*, 697.
[7] L. Tiefenauer, C. Padeste, *Chimia* **1999**, *53*, 62.
[8] O. Niwa, K. Hayashi, R. Kurita, T. Horiuchi, *Mater. Integr.* **2002**, *15*, 17.
[9] S. Shoji, T. Ohori, H. Kawashima, K. Miura, A. Yotsumoto, *Proc.—Electrochem. Soc.* **1997**, *97-5*, 12.
[10] B. Xie, K. Ramanathan, B. Danielsson, *TrAC, Trends Anal. Chem.* **2000**, *19*, 340.
[11] K. Hayashi, R. Kurita, T. Horiuchi, O. Niwa, *Chem. Sens.* **2001**, *17*, 97.
[12] Y. Jiang, P. Wang, L. E. Locascio, C. S. Lee, *Anal. Chem.* **2001**, *73*, 2048.
[13] C. J. H. Brenan, K. Domansky, P. Kurzawski, L. G. Griffith, *Proc. SPIE—Int. Soc. Opt. Eng.* **2000**, *3912*, 76.
[14] C. B. Freidhoff, R. M. Young, S. Sriram, T. T. Braggins, T. W. O'Keefe, J. D. Adam, H. C. Nathanson, R. R. A. Syms, T. J. Tate, M. M. Ahmad, S. Taylor, J. Tunstall, *J. Vac. Sci. Technol., A* **1999**, *17*, 2300.
[15] C.-F. Yeh, Y.-C. Lee, J.-L. Su, *Proc. SPIE—Int. Soc. Opt. Eng.* **1996**, *2879*, 260.
[16] G. Wulff, *Angew. Chem., Int. Ed. Engl.* **1995**, *34*, 1812.
[17] K. J. Shea, *Trends Polym. Sci.* **1994**, *2, 166.*
[18] M. J. Whitecombe, E. N. Vulfson, *Adv. Mater.* **2001**, *13*, 467.
[19] K. Haupt and K. Mosbach, *Chem. Rev.* **2000**, *100*, 2495.
[20] B. Sellergren, *Molecularly Imprinted Polymers: Man-Made Mimics of Antibodies and Their Applications in Analytical Chemistry*, Vol. 23, Elsevier, New York **2001**.
[21] M. Yan, A. Kapua, *Anal. Chim. Acta* **2001**, *435*, 163.
[22] G. M. Whitesides, E. Ostuni, S. Takayama, X. Jiang, D. E. Ingber, *Annu. Rev. Biomed. Eng.* **2001**, *3*, 335.
[23] G. Vozzi, C. J. Flaim, F. Bianchi, A. Ahluwalia, S. Bhatia, *Mater. Sci. Eng., C* **2002**, *20*, 43.
[24] X. Zhang, X. N. Jiang, C. Sun, *Sens. Actuators, A* **1999**, *77*, 149.
[25] S. Kawata, H. B. Sun, T. Tanaka, K. Takada, *Nature* **2001**, *412*, 697.
[26] K. Ikuta, K. Hirowatari, *Proc.—IEEE Micro Electro Mech. Syst.* **1993**, 42.
[27] C. Sun, X. Zhang, *J. Appl. Phys.* **2002**, *92*, 4796.
[28] P. F. Jacobs, *Rapid Prototyping and Manufacturing: Fundamentals of Stereolithography*, Society of Manufacuring Engineers, Dearborn, MI **1992**.
[29] K. J. Shea, D. A. Spivak, B. Sellergren, *J. Am. Chem. Soc.* **1993**, *115*, 3368.
[30] D. A. Spivak, M. A. Gilmore, K. J. Shea, *J. Am. Chem. Soc.* **1997**, *119*, 4388.
[31] D. A. Spivak, K. J. Shea, *Macromolecules* **1998**, *31*, 2160.
[32] A. Guyot, M. Bartholin, *Prog. Polym. Sci.* **1982**, *8*, 227.
[33] *Synthetic Procedures in Nucleic Acid Chemistry*, Vol. 1, 2 (Eds: W. W. Zorbach, R. S. Tipson), Interscience, New York **1968**.

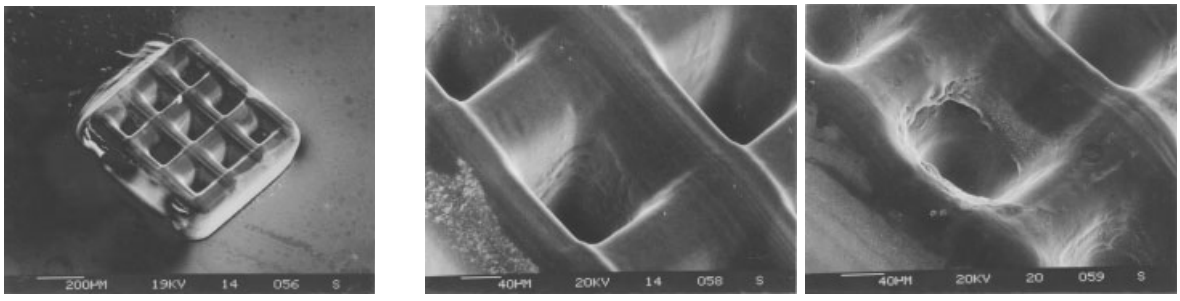

(a) (b)

Fig. 3. a) SEM image of a 3D imprinted microstructure (600 μm × 600 μm × 100 μm). b) Close-ups of the structure show the wall thickness to be approximately 10 μm.

